Global NEST Journal, Vol 27, No 3, 06838

The impact of formulation and process variables on the formation of chitosan-alginate and chitosan-pectin nanoparticles

Uce Lestari[1,2], Muhaimin Muhaimin[3]*, Anis Yohana Chaerunisaa[4] and Wawan Sujarwo[5]

[1]Doctoral Program, Faculty of Pharmacy, Universitas Padjadjaran, Jalan Raya Jatinangor Km 21.5, Jatinangor, West Java, 45363, Indonesia

[2]Department of Pharmacy, Faculty of Medicine and Health Sciences, University of Jambi, Jalan Jambi-Muara Bulian Km 15, Mendalo Darat, Jambi Luar Kota, Muaro Jambi, Jambi, 36361, Indonesia

[3]Department of Pharmaceutical Biology, Faculty of Pharmacy, Universitas Padjadjaran, Jalan Raya Jatinangor Km 21.5, Jatinangor, West Java, 45363, Indonesia

[4]Department of Pharmaceutics and Pharmaceutical Technology, Faculty of Pharmacy, Universitas Padjadjaran, Jalan Raya Jatinangor Km 21.5, Jatinangor, West Java, 45363, Indonesia

[5]Research Center for Ecology and Ethnobiology, National Research and Innovation Agency (BRIN), Cibinong, Bogor, West Java, 16911, Indonesia

Received: 26/09/2024, Accepted: 13/01/2025, Available online: 14/01/2025

*to whom all correspondence should be addressed: e-mail: muhaimin@unpad.ac.id

https://doi.org/10.30955/gnj.06838

Graphical abstract

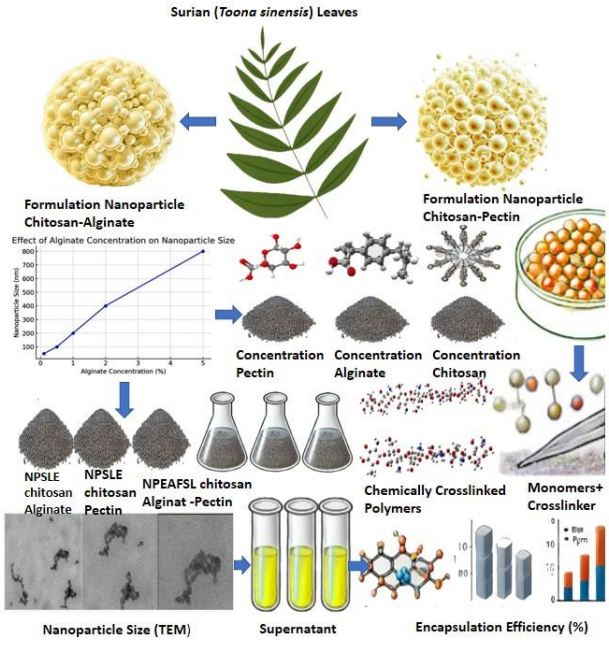

Abstract

Chitosan-alginate and chitosan-pectin nanoparticles show great promise as delivery systems in cosmetics. To optimize efficiency of natural polymer utilization, we implemented a development approach for chitosan-alginate and chitosan-pectin nanoparticles, aiming to enhance their activity and stability compared to their extract forms. Through ionic gelation, nanoparticles from Surian leaf extract (SLE) and ethyl acetate fraction of Surian leaf (EAFSL) were formed with particle sizes ranging from 172 nm to 200 nm, polydispersity index (PI) ranging from 1.3 to 1.9, and zeta potential ranging from -11 mV to -27 mV. Utilization of alginate polymer affects activity of SLE and EAFSL nanoparticles in inhibiting elastase enzymes. In inhibition tests against elastase enzyme, it was found that chitosan-alginate and chitosan-pectin polymers exhibited the highest % inhibition compared to SLE and EAFSL alone. SLE nanoparticles with 0.75% chitosan and 1.25% alginate polymers showed a % inhibition of 39.40% against elastase enzyme, whereas SLE alone exhibited only 30.18% inhibition. While, EAFSL nanoparticles with 0.75% chitosan and 1.25% alginate polymers demonstrated an 87.30% inhibition against elastase enzyme, compared to EAFSL alone with only 22.42% inhibition. SLE and EAFSL nanoparticles with chitosan-alginate and chitosan-pectin polymers increase in inhibiting elastase enzymes compared to SLE and EAFSL alone.

Keywords: chitosan-alginate, chitosan-pectin, nanoparticles, ionic gelation, elastase enzyme.

1. Introduction

The use of natural polymers such as chitosan, alginate, and pectin in nanoparticle production has become the primary choice. This is due to their unique properties that are well-suited for their respective applications (Kurl *et al*. 2023; Yubia *et al*. 2021). Chitosan is derived from chitin, commonly found in the exoskeletons of arthropods such as crabs, crayfish, shrimp, and lobsters. The concentration of chitosan typically ranges from 0.1% w/v to 2% w/v, depending on the production method and intended application. Alginate is a polymer extracted from brown algae (Kurl *et al*. 2023; Yubia *et al.* 2021). The commonly used concentration of alginate ranges from 0.5% to 3%. Meanwhile, pectin is extracted from fruits and vegetables, with the usual concentration ranging from 0.1% to 1%. The

concentration of these natural polymers plays a crucial role in determining the particle size, morphology, and stability of the resulting nanoparticles (Yubia *et al*. 2021). Choosing the appropriate concentration for each polymer allows for the adjustment of the physicochemical properties of the nanoparticles, supporting their successful application in pharmaceuticals, drug delivery, and various other industries (Kurl *et al*. 2023; Yubia *et al*. 2021).

The use of natural polysaccharides or hydrophilic polymers mentioned above as drug carriers or active substances has been the main focus in the development of innovative drug delivery systems (Javid *et al.* 2024). Chitosan possesses hydrophilic properties that allow the formation of a polymer matrix capable of efficiently containing drugs. Apart from that, alginate, with its hydrophilic nature, can form hydrogels when interacting with calcium ions (Javid *et al*. 2024; Wani *et al.* 2023). This enables sustained and controlled release of the active substance over the desired period. Furthermore, pectin can be used to form an environmentally friendly hydrophilic matrix. The advantages of these three hydrophilic or natural polymers, such as biodegradability and biocompatibility, make them ideal as drug carriers in medical and pharmaceutical applications (Wani *et al*. 2023). Through careful and precise formulation, these natural hydrophilic polymers can enhance the stability and effectiveness of drug delivery, making them a promising primary choice in the development of innovative and efficient drug delivery systems (Wani *et al*. 2023; Meng *et al*. 2024) .

Natural polymers or hydrophilic substances such as chitosan, alginate, and pectin have both advantages and disadvantages in their roles as drug carriers or active substances (Meng *et al*. 2024). Their advantages include hydrophilic properties that facilitate excellent interaction with water, allowing controlled and slow drug release. For instance, chitosan can form a stable polymer matrix, enhancing drug bioavailability. Alginate can form hydrogels enabling gradual drug release, while pectin, with its gelling property, provides effective release control (Medha and Sethi. 2024). However, their weaknesses encompass limited mechanical stability, restricting their application in certain contexts. Additionally, they are highly sensitive to environmental factors, such as specific pH levels or ion content, which can influence the characteristics of these drug carriers. Therefore, the careful selection of these natural polymers or hydrophilic substances, along with precise formulation design, is crucial to maximize benefits and overcome limitations in the development of an effective drug delivery system control (Medha and Sethi. 2024; Mondal *et al.* 2023).

Natural polymers such as chitosan, alginate, and pectin, originating from natural sources, have garnered significant attention in the pharmaceutical industry. Chitosan serves as an efficient and stable drug carrier, contributing to the improvement of solubility and bioavailability of active substances (Mondal *et al.* 2023; Afzal *et al.* 2023). Alginate is employed in drug formulations with controlled release mechanisms, while pectin is commonly used in creating hydrophilic matrices for orally disintegrating drug delivery. The utilization of these natural polymers in the pharmaceutical industry reflects a push toward developing safer and more effective drug delivery systems. There is an increased emphasis on environmentally friendly and biodegradable materials in this pursuit (Mondal *et al.* 2023; Afzal *et al.* 2023).

These natural polysaccharide polymers hold significant applications in biomedical contexts. For example, chitosan is widely used in the production of drug-delivery materials and medical devices due to its highly biocompatible nature (Afzal *et al*. 2023). Chitosan has also shown potential in wound healing processes and tissue regeneration. Alginate, with its ability to form hydrogels, can be applied in constructing matrices for drug delivery, cell therapy, and tissue expansion (Yu *et al.* 2024). Furthermore, pectin, with its gelling properties, is widely employed in formulating orally disintegrating drugs and matrix-based delivery systems. Overall, these natural polymers play a crucial role in the development of biomedical technology, providing innovative solutions for controlled drug delivery, tissue regeneration, and other therapeutic applications in the context of health and medical care (Pires-Patricia *et al*. 2023)

One of the most extensively researched and adopted methods for nanoparticle production is the polymer nanoparticle synthesis through the ionic gelation method. The ionic gelation method has gained intense attention, particularly in the context of biomedical applications. Ionic gelation involves the use of a polymer solution and an ion acting as a gelling agent, such as calcium or zinc (Qureshi *et al*. 2019). This process leverages the ionic interaction between the gelling agent and the polymer, resulting in a gel structure that can be utilized for nanoparticle formation. The development of this method has been a focal point of research due to its ability to produce nanoparticles with precisely controlled sizes and properties (Veiga *et al.* 2023). Further research in the ionic gelation method focuses on optimizing parameters such as solution concentration, the ratio of gelling agent ions to the polymer, and gelation conditions to yield nanoparticles with optimal performance and stability. The success of this method in producing nanoparticles with high control has propelled various applications across different fields, including drug delivery and biomedical diagnostics (Balde *et al*. 2023).

In addition to the ionic gelation method, another method that has gained attention in nanoparticle production is the emulsification and solvent dissolution method. This method involves using an organic solvent that is compatible with the desired raw materials, such as polymers or biologically active compounds. This solvent is then emulsified in the aqueous phase or a carrier solution containing emulsifying agents, creating nanoparticles on a nanometer scale (Sharma *et al.* 2023). Subsequently, an evaporation or drying process is conducted to remove the solvent, yielding nanoparticles applicable in various applications, including drug delivery. This approach allows for good control over the size, distribution, and morphology of nanoparticles, which are key factors in

enhancing the efficiency of drug delivery and the bioavailability of active substances. Despite the various variations in this method, research conducted by different scientific groups has shown that the emulsification and solvent dissolution method can be flexibly adapted for the production of nanoparticles tailored to specific needs in various applicative contexts (Sharma *et al.* 2023; Sindhu *et al*. 2022).

Lastly, the most recently researched and widely adopted method for nanoparticle production is polymer nanoparticle synthesis through the nanoprecipitation technique. This method involves blending an organic polymer solution with a non-solvent, leading to spontaneous precipitation and the formation of nanoparticles (Desu *et al*. 2022). This technique provides precise control over the size and distribution of particles by adjusting the ratio between the polymer solution and non-solvent, polymer concentration, and other parameters. Additionally, the nanoprecipitation method tends to be environmentally friendly as it does not require excessive use of hazardous organic solvents. Consequently, this method is extensively applied in developing drug delivery systems, particularly to enhance drug solubility and facilitate controlled release (Rani *et al.* 2023). Ongoing research aims to comprehend and enhance this method, ensuring its broad applicability in various fields, including health and technology (Sindhu *et al*. 2022).

In this study, the ionic gelation method was utilized because it offers significant advantages in nanoparticle production compared to other methods when combined with natural polymers like chitosan, alginate, and pectin, using the NaTPP (sodium tripolyphosphate) as a cross-linker (Sindhu *et al.* 2022). Natural polymers such as chitosan, alginate, and pectin possess biodegradable and biocompatible properties, making the resulting nanoparticles more environmentally friendly and safe for biomedical applications (Jiang *et al.* 2024). Ionic gelation allows for efficient and controlled nanoparticle formation, resulting in uniform particle size and perfect distribution. The use of the NaTPP cross-linker enhances the structural stability of nanoparticles, making them more resistant to environmental changes and providing mucoadhesive properties that strengthen interactions with target cells (Balde *et al.* 2023). This method ensures better control over the physicochemical properties of nanoparticles, enabling broader applications in drug delivery, gene therapy, and other fields (Desu *et al.* 2022).

This research aims to investigate the influence of formulation variables, particularly the types and concentrations of polymers, on the formation of chitosan-alginate and chitosan-pectin nanoparticles (Wang *et al.* 2024). In terms of formulation aspects, this study delves into how variations in polymer types (chitosan, alginate, and pectin) and changes in the concentration of each polymer can affect the physicochemical properties of the resulting nanoparticles. This includes particle size, polydispersity index (PI), zeta potential, encapsulation efficiency (% EE), and stability during storage (Yu *et al.* 2024). Additionally, the research aims to understand the impact of formulation variables on the morphology of nanoparticles and their potential application as anti-aging agents by assessing their inhibitory activity against elastase enzymes. By focusing on the influence of polymer types and concentrations in the formulation, it is expected that this study will provide deeper insights to optimize the design of chitosan-alginate and chitosan-pectin nanoparticles for anti-aging purposes.

2. Materials and methods

2.1. Collection of plant materials

Fresh leaves of surian (*Toona sinensis*) were collected in the month of October, 2022 from Rantau Suli Village, East Jangkat, Merangin Regency, Jambi Province, Indonesia and identified by a taxonomist (Dr. Silva Abraham) from the Directorate of Scientific Collection Management of the National Research and Innovation Agency in Central Jakarta, where voucher specimen (No. B-4601/II.6.2/DI.05.07/12/2022) was deposited. The fresh leaves were washed thoroughly to remove dirt and soil, then dried and stored at room temperature. These leaves were grinded and then kept in closed container and stored at room temperature until they will be used for the next process. Information about the plant, the location and date of collection were stated in the Directorate of Scientific Collection Management of the National Research and Innovation Agency in Central Jakarta.

2.2. Materials and equipment

Other materials included ethanol 70% (Brataco), chitosan (Harum Kimia), alginate (Harum Kimia), pectin (Kisbiokim Medilab), NaTPP or sodium tripolyphosphate (Brataco), acetic acid 98% (Brataco), aluminum chloride (Brataco), sodium acetate (Brataco), methanol p.a. (Merck), AQUA PRO Injection (Kimia Farma), and distilled water or Aquadest (Kisbiokim Medilab).

Apart from that, the equipment used in this research included a rotary evaporator (Heidolph), hot plate magnetic stirrer (Thermo Fisher Scientific), particle size analyzer (Horiba Scientific SZ-100), UV-vis spectrophotometer (Specord), micro pipet 10-100 µL (Acura 825), pH meter (Hanna Instruments), micropump (China), centrifuge (Labnet), transmission electron microscopy (Tecnai G2 20 S-Twin Function), ELISA microplates, and plasticware (Thermo Fisher Scientific). Figure 1 shows the flow chart of research process and methods.

2.3. Surian leaf extract (SLE)

The simplicia extraction of Surian leaves was conducted using the maceration method with ethanol 70% as the solvent. The process for extracting Surian leaves is outlined as follows: 5.98 kg of Surian leaf simplicia was weighed and placed into the macerator. Ethanol 70% was added until all Surian leaf simplicia was fully submerged, with a ratio of 1 part Surian leaf simplicia powder (5.98 kg) to 10 parts ethanol 70% solvent (60 liters). The mixture was left to stand for 24 hours. The obtained liquid extract was collected, resulting in 45 liters of macerate. Subsequently, an equal amount of ethanol 70% was added back into the

macerator. The extraction process was repeated for three cycles of 24 hours each. The liquid extract obtained was then concentrated using a rotary evaporator at 50°C. The extract was further concentrated using a water bath at 50°C until a concentrated Surian leaf extract was obtained, and the extraction yield value was calculated (Taslim *et al.* 2020).

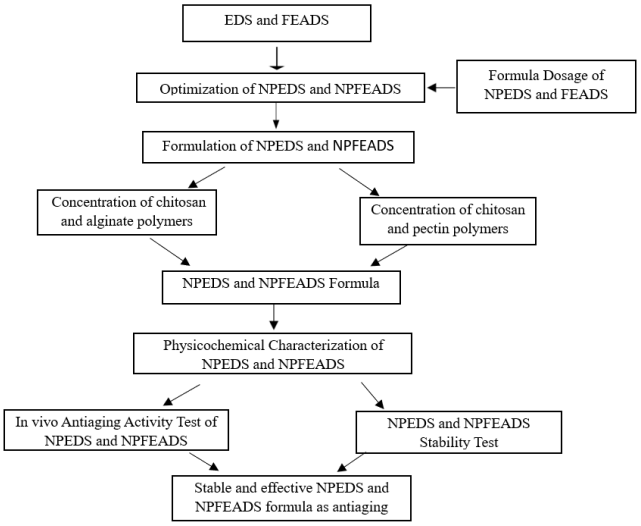

Figure 1. Flow chart of research process and methods

2.4. Ethyl acetate fraction of Surian leaves (EAFSL)

The fractionation of Surian leaf extract was conducted using the liquid-liquid extraction (LLE) method with three solvents of different polarities: n-hexane, ethyl acetate, and water. The fractionation process of Surian leaves is as follows: 50 g of Surian leaf extract was weighed and then ground with 400 mL of n-hexane in a mortar. The resulting filtrate was poured into a separating funnel until the n-hexane solvent was depleted. An equal amount of water was added, and the mixture was shaken for 15 minutes with occasional venting of air from the funnel every 5 minutes. The mixture in the separating funnel was allowed to stand until the two solvents separated thoroughly for 24 hours. The n-hexane fraction was separated from the water fraction. The separation process was repeated until an almost colorless n-hexane fraction was obtained. An equal amount of ethyl acetate was added to the same separating funnel, shaken, and separated following the previous procedure. The n-hexane, ethyl acetate, and water fractions were concentrated using a rotary evaporator at 50°C. The n-hexane, ethyl acetate, and water fractions were further concentrated using a water bath at 50°C to obtain the concentrated n-hexane, ethyl acetate, and water fractions of Surian leaves (Cahyani *et al*. 2018).

2.5. Formulations for SLE and EAFSL nanoparticles

The preparations of Surian leaf extract (SLE) nanoparticles and ethyl acetate fraction of Surian leaves (EAFSL) nanoparticles were carried out using the ionic gelation method with three formulations utilizing chitosan and alginate polymers, and additionally, three formulations using chitosan and pectin polymers. The SLE concentration was 1.4 mg/mL (1400 ppm), while EAFSL had a concentration of 1.8 mg/mL (1800 ppm), both utilizing the NaTPP as a cross-linker. The formulations for SLE and EAFSL nanoparticles are presented in Tables 1 and 2 below.

Table 1. SLE nanoparticle formulations

Ingredients	F IA-E	F IIA-E	F IIIA-E	F IP-E	F IIP-E	F IIIP-E	Functions
SLE (%)	0.14	0.14	0.14	0.14	0.14	0.14	Active substance
Chitosan (%)	1	0.75	1.25	1	0.75	1.25	Natural polymer (polycation)
Alginate (%)	1	1.25	0.75	-	-	-	Natural polymer (enteric)
Pectin (%)	-	-	-	0.5	0.75	0.25	Natural polymer (enteric)
NaTPP (%)	0.7	0.7	0.7	0.7	0.7	0.7	Cross-linker (polyanion)
Acetic acid + distilled water (ml) ad	310	310	310	310	310	310	Solvent

Table 2. EAFSL nanoparticle formulations

Ingredients	F IA-F	F IIA-F	F IIIA-F	F IP-F	F IIP-F	F IIIP-F	Functions
EAFSL (%)	0.18	0.18	0.18	0.18	0.18	0.18	Active substance
Chitosan (%)	1	0.75	0.5	1	0.75	0.5	Natural polymer (polycation)
Alginate (%)	1.5	1.25	1	-	-	-	Natural polymer (enteric)
Pectin (%)	-	-	-	0.875	0.625	0.375	Natural polymer (enteric)
NaTPP (%)	0.7	0.7	0.7	0.7	0.7	0.7	Cross-linker (polyanion)
Acetic acid + distilled water (ml) ad	310	310	310	310	310	310	Solvent

2.6. Preparation of SLE and EAFSL nanoparticles

The preparation of SLE and EAFSL nanoparticles began by dissolving SLE in ethanol solvent with a concentration of 28 mg/20 ml (SLE was weighed at 28 mg and added to 20 ml of ethanol, and the mixture was homogenized) for each respective formula. For the preparation of EAFSL nanoparticles, EAFSL was dissolved in ethanol solvent with a concentration of 36 mg/20 ml (EAFSL was weighed at 36 mg and added to 20 ml of ethanol, and the mixture was homogenized) for each respective formula. Chitosan was weighed according to the concentration specified in the above formulas and dissolved in acetic acid with a total volume of 200 ml. Chitosan was added gradually to the acetic acid 2% solution and stirred with a magnetic stirrer until chitosan was completely dissolved. The pH was checked until it reached pH 4. In addition, alginate was weighed according to the concentration specified in the formulas F IA-E, F IIA-E, F IIIA-E, F IA-F, F IIA-F, and F IIIA-F. It was then dissolved in 50 ml of distilled water (Aquadest) and stirred until homogeneous. The pH was checked until

it reached 6.5. Furthermore, pectin was weighed according to the concentration in the formulas F IP-E, F IIP-E, F IIIP-E, F IP-F, F IIP-F, and F IIIP-F. It was dissolved in 50 ml of distilled water (Aquadest), stirred until homogeneous, and the pH was checked until it reached 5. Additionally, NaTPP was weighed at 28 mg, added to 40 ml of distilled water (Aquadest) for each formula mentioned above, stirred homogeneously, and the pH was checked until it reached 3.6 (Deniz *et al.* 2019).

The dissolved SLE and EAFSL were mixed with chitosan (mass 1). A micropump device consisting of 2 magnetic stirrers was prepared. On the left side, there was a solution of SLE, EAFSL, and chitosan (mass 1), and on the right side, there was a solution of NaTPP (mass 2). The principle of the micropump was that mass 1 would pass through the micropump drop by drop into mass 2 until the mass 1 solution was completely transferred to mass 2. Once mass 1 was depleted, the micropump was turned off. Mass 3 (SLE, EAFSL, and chitosan added to NaTPP) was transferred to another magnetic stirrer, and then alginate and pectin were added according to the above formulas, drop by drop, at a speed of 1000 RPM for 1 hour at 40°C (Gul *et al*. 2024).

2.7. Characterization of the physical-chemical properties of SLE and EAFSL nanoparticles

The physical-chemical properties of SLE and EAFSL nanoparticles were examined, including organoleptic characteristics, pH, sedimentation degree, % EE (encapsulation efficiency percentage), and surface morphology of the nanoparticles. The observation of organoleptic properties aims to evaluate the sensory characteristics of nanoparticles, such as color, odor, taste, shape, and consistency observed visually. This is intended to ensure the quality of nanoparticles and assist in the development and improvement of nanoparticle formulations (Vithoba *et al.* 2023).

The examination of nanoparticle morphology was conducted using negative staining transmission electron microscopy (TEM). In summary, a drop of the sample, diluted with water to approximately 0.05 mg/mL, was placed on a Formvar copper mesh 200. It was allowed to adsorb, and the excess was removed using filter paper. A drop of uranyl acetate 2% solution (w/v) was added and allowed to contact the sample for 5 minutes. Excess water was removed, and the sample was air-dried before vesicles were observed using TEM operating at 200 KV (Kumar *et al*. 2024).

For the % EE (encapsulation efficiency percentage) of SLE nanoparticles, 28 mg/20 ml of samples were centrifuged at 12000 rpm for 60 minutes at 40°C. The concentration of the free drug (in the supernatant, 1.5 ml) was determined by measuring the quercetin content in the supernatant using a UV-vis spectrophotometer at a previously specified maximum wavelength (i.e., 426 nm) (Tian *et al*. 2024).

$$\%EE = \frac{\text{Total flavonoid content in SLE} - \text{Total flavonoid content in supernatant}}{\text{Total flavonoid content in SLE}} \times 100\%$$

2.8. Characterization of SLE and EAFSL nanoparticles

The characterization of nanoparticles was conducted to ensure the quality of the produced nanoparticles. The quality was observed through particle size, polydispersity index (PI), zeta potential value, and the percentage of encapsulation efficiency (% EE) (Vithoba *et al.* 2024).

Particle size and PI examinations were carried out using the particle size analyzer (PSA) with the dynamic light scattering (DLS) method. Furthermore, the zeta potential was determined using the Zetasizer Zen3600 with a 10-fold sample dilution in an aqueous medium at room temperature (Deniz *et al*. 2019).

2.9. Determination of the activity and inhibition of the anti-elastase enzyme

The activity of the anti-elastase enzyme was assessed using the neutrophil elastase inhibitor screening kit method. The process began by preparing the solution, as follows:[20] SLE with a concentration of 1.4 mg/mL was dissolved in DMSO solvent. It was then diluted up to four times the desired final test concentration with assay buffer. Subsequently, 25 microliters of each diluted test compound were added to separate wells of a 96-well plate. The various SLE nanoparticle formulas that had been prepared were also included (Desmiaty *et al*. 2020).

Inhibitor control stock 1:25 was diluted with assay buffer, and 25 microliters of the diluted inhibitor control were added to separate wells of the plate. An additional 25 microliters of assay buffer were added to separate the wells on the plate. It should be noted that enzyme controls needed to be set each time the test was conducted. Finally, 75 microliters of assay buffer were added to separate the wells on the plate. For each well (except the background control well), 50 microliters of neutrophil elastase solution were prepared according to Table 3.

Table 3. Reagent volumes for neutrophil elastase solution preparation

Reagent	Volume
Assay buffer	48 microliters
Neutrophil elastase stock solution	2 microliters

50 microliters of diluted neutrophil elastase solution were added to each well labeled as test compound, inhibitor control, and enzyme control. Background control wells were not added. The plate was mixed thoroughly and incubated for 5 minutes at 37°C. The plate was protected from light during incubation. The volume in all wells—including test compounds, inhibitor control, enzyme control, and background control at this step—was 75 microliters (Desmiaty *et al.* 2020).

A sufficient amount of reagent for the intended number of tests was prepared. 25 microliters of the reaction mixture were prepared for each well according to Table 4.

Table 4. Components and volumes of the reaction mixture for enzyme activity assessment

Reagent	Working reagent
Assay buffer	23 microliters
Substrate	2 microliters

25 microliters of the reaction mixture were added to each reaction container—including test compound, inhibitor

control, enzyme control, and background control. The plate was mixed, and measurements were taken immediately (Desmiaty *et al*. 2020).

Fluorescence (relative fluorescence unit [RFU]) was measured at λ Ex = 400 nm / λ Em = 505 nm in the microplate. It was read in kinetic mode for 30 minutes at 37°C. The plate was protected from light during incubation. It was recommended to read fluorescence every following minute: 0, 10, 20, and 30 minutes. After obtaining the encapsulation values, calculations were performed for % elastase enzyme activity against the test compound and % elastase enzyme inhibition against the test compound using the following formulas:

$$\%\text{Activity} = \frac{\Delta\text{RFU Test Compound}}{\Delta\text{RFU Enzyme Control}} \times 100\%$$

$$\%\text{Inhibition} = 1 - \left(\frac{\Delta\text{RFU Test Compound}}{\Delta\text{RFU Enzyme Control}} \right) \times 100\%$$

Then, a graph depicting the profile of neutrophil elastase (NE) activity was generated with different concentrations of the test compound. Additionally, a graph illustrating the relationship between % activity values and % inhibition values of the test compound was also created.

2.10. Short-term stability test at room temperature for 2 months

The objective of the short-term stability test at room temperature is to assess how well nanoparticles can preserve their quality during storage. Parameters monitored during room temperature storage include % EE (encapsulation efficiency), pH, sedimentation degree, and characterization throughout the storage period (Zhu *et al*. 2024).

Table 5. Characterization of specific and non-specific parameters of simplicia and Surian Leaf Ethanol Extract (SLE)

No	Parameters	Data		Reference
		Simplicia	SLE	
1	Rendement	53.36%	33.28%	Simpilicia ≥ 20% extract ≥ 7.2%.
2	pH	5.18	4.46	4-6
3	Water soluble essence	21%	59,30%	≥ 18%
4	Ethanol soluble essence	21%	67.50%	≥ 6.30%
5	Density	0.66	1.55	-
6	Total ash content	5.33%	2.64%	≤ 10%
7	Acid insoluble ash content	1.13%	0.40%	≤ 2,60%
8	Water soluble ash content	25%	17.50%	≥ 18%
9	Ethanol soluble ash content	47.50%	15%	≥ 6,30%
10	Water content	8.3%	8.18%	≤ 10%
11	Drying shrinkage	5.50%	12.68%	≤ 11%
12	Microbial contamination or ALT	-	< 10 cfu/gr	< 10 cfu/gr
13	Mold contamination	-	< 10 cfu/gr	< 10 cfu/gr
14	Pb contamination	-	0.28 mg/kg	It should not be more than 20 mg/kg
15	Cu contamination	-	16.95 mg/kg	0.1 – 150 mg/kg
16	Cd contamination	-	0.2 mg/kg	It should not be more than 5 mg/kg
17	Zn contamination	-	4.75 mg/kg	2.0 - 100 mg/kg
18	Total flavonoid content	-	33.19 mg/g	-
19	Total phenolic content	-	153.10 mg/g	-

2.11. Data analysis

The experimental results included three replications, and the data were expressed as mean ± standard deviation (SD). The data were analyzed by an ANOVA ($p < 0.05$) using SPSS, and $p < 0.05$ was considered to be statistically significant, which means that there is an effect of variations in the concentration of chitosan alginate polymer and chitosan pectin polymer in each nanoparticle formula.

3. Results and discussion

3.1. Extraction and fractionation of Surian leaves

The ethanol extract from Surian leaves was obtained in the amount of 1.99 kg from an initial raw material weight of 5.98 kg. In this study, the extract yield was found to be 33.28%, exceeding the expected 7.20%. Meanwhile, the yield of the ethyl acetate fraction from Surian leaves was 0.53%, falling short of the expected 7.20% as per the Herbal Pharmacopoeia. Yield is a crucial parameter in evaluating the efficiency of an extraction method. The higher the yield is, the more efficient the extraction method will be in isolating the desired compounds. Additionally, the extract yield plays a significant role in determining the economic value of a natural substance, as it can influence the availability and price of the material. Therefore, extract yield becomes a key factor in optimizing the extraction process and maximizing the benefits of the natural material used. The low yield of the ethyl acetate fraction is attributed to the incomplete fractionation of the entire extract (Magdassi *et al.* 1997; Patravale *et al.* 2008).

Based on research by Lestari et al, 2023c, the simplicia and Surian Leaf Ethanol Extract (SLE) used have met the requirements for testing specific and non-specific parameters as in Table 5 below:

3.2. Production of SLE and EAFSL nanoparticles

The latest developments for antiaging nanodelivery using plant extracts, one of which is the ethanol extract of surian leaves (SLE) which has a total phenolic content of 153.10 mg/g and a total flavonoid content of 33.19 mg/g with an IC50 value of 12.35 ppm indicating its antioxidant activity is very strong. Based on previous studies, the most active fraction among the n-hexane fraction, water fraction and ethyl acetate fraction is the ethyl acetate fraction of surian leaves (EAFSL) with an IC50 value of 15.59 ppm which has very strong antioxidant activity (Lestari *et al.* 2023c), so SLE and EAFSL were chosen to be further developed into a nanotechnology-based system for the delivery of herbal antiaging therapy with better bioavailability. This nanoparticle system is expected to increase activity as an antiaging, so that less active substance is needed because of the increased absorption of the active substance itself (Lestari *et al*. 2023c).

Based on previous study, SLE with a concentration of 1.4 mg/ml has the greatest inhibitory activity against the elastase enzyme of 30.18% compared to SLE with a concentration of 1.8 mg/ml; 1.0 mg/ml and 0.6 mg/ml while EAFSL with a concentration of 1.8 mg/ml has the greatest inhibitory activity against the elastase enzyme of 22.42% compared to EAFSL with a concentration of 1.4 mg/ml; 1.0 mg/ml and 0.6 mg/ml, as well as against FnHSL (n-hexane fraction of surian leaves) and FWSLE (water fraction of surian leaves) with various concentrations.

The development of nanoparticles derived from natural products, such as ethanol extract from Surian leaves, in drug delivery systems is currently an innovative and promising trend in the fields of pharmacy and medicine (Lestari *et al*. 2023a). This utilization of natural resources not only reduces dependence on synthetic chemicals but also harnesses the therapeutic potential of various active compounds present in the plant extract (Lestari *et al.* 2023b). Nanoparticles created from plant extracts, like the ethanol extract from Surian leaves, offer several advantages, including high biocompatibility, potent antioxidant potential, synergistic anti-aging activity, and the ability to interact with biological cells. Moreover, the biodegradable nature of some plant extracts allows for a reduction in harmful environmental impact (Lestari *et al.* 2023c). The application of these nanoparticles in drug delivery systems opens up opportunities to enhance bioavailability, stability, and target delivery, thereby improving their efficacy. With the ongoing progress in this research field, it is expected that more efficient and safe formulations will be discovered, making the use of nanoparticles from natural products a promising option for the development of advanced and environmentally friendly drug therapies (Lestari *et al*. 2023a).

Based on the results of the SLE and EAFSL research, SLE has an IC_{50} of 12.35 ppm and EAFSL has 15.59 ppm. Vitamin C, as the positive control, was measured at 7.81 ppm. The IC_{50} results for SLE and EAFSL are close to the positive control of Vitamin C, categorizing them as having very strong antioxidant properties because IC_{50} is < 50 ppm. This antioxidant activity works synergistically in stabilizing the role of reactive oxygen species (ROS) in the photoaging process. Thus, the ethanol extract and the active fraction of Surian leaves (*Toona sinensis*) can be developed in nanoparticle form (Lestari *et al.* 2023d).

In this study, polymeric SLE and EAFSL nanoparticles based on chitosan with sodium tripolyphosphate cross-linking agent, subsequently coated with alginate and pectin, are formulated to enhance anti-aging activity. The formulation scheme for this research is illustrated in the Figure 2 below.

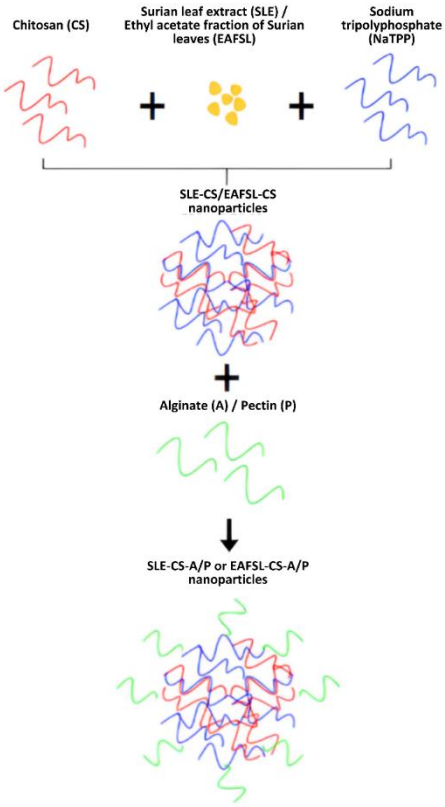

Figure 2. Scheme of chitosan-based SLE and EAFSL nanoparticle formulation coated with alginate and pectin

The reason for adding sodium tripolyphosphate (NaTPP) cross-linker is because NaTPP is negatively charged and has three free groups to interact with the amine group ($-NH3^+$) in the chitosan polymer so that the higher the concentration, the greater the number of chitosan chains attached to the volume of the nanoparticles, so that the particles produced after the ionic gelation process become larger. NaTPP also has the ability to produce nanoparticles with uniform particle distribution and size so that it can increase the stability of the nanoparticle structure during storage. Therefore, the choice of NaTPP cross-linker is very appropriate for drug delivery systems in the form of nanoparticles (Milenkova *et al*. 2024).

The production of polymeric SLE and EAFSL nanoparticles was conducted using the ionic gelation method. Physical cross-linking through electrostatic interactions, as an alternative to chemical cross-linking, has been implemented to avoid potential toxicity from reactants and other undesired consequences. The mechanism of chitosan nanoparticle formation with this method is based on the positive charge of the amino groups ($-NH_3^+$) in chitosan

interacting with the negative charge of the phosphate groups (PO_4^{3-}) from the crosslinking agent (i.e., sodium tripolyphosphate). Due to the complexation between these different charges, chitosan undergoes ionic gelation and successfully forms spherical particles. Thus, the nanoparticles are spontaneously formed due to mechanical stirring at room temperature (Arozal *et al.* 2021; Chiesa *et al.* 2008).

The mechanism of coating chitosan-based nanoparticles with alginate and pectin relies on the interaction between the amino groups on chitosan, functioning as positive charge donors ($-NH_3^+$), on the nanoparticle surface, and the carboxyl groups on alginate and pectin, serving as negative charge donors (COO^-). This interaction facilitates the formation of cationic bonds between chitosan and alginate, as well as chitosan and pectin, providing stability and mechanical strength to the resulting nanoparticle structure (Kalam *et al.* 2016). A critical step in the surface coating of SLE and EAFSL nanoparticles using alginate and pectin (polyelectrolytes) is the inversion of the zeta potential of the nanoparticles. This inversion is crucial as agglomeration is likely to occur around the isoelectric point. The isoelectric point may influence the surface properties of the nanoparticles and can play a role in the nanoparticle agglomeration process. Agglomeration happens due to interactions between positively and negatively charged components on different nanoparticles or due to the absence of electrostatic stabilization during the intermediate stage of encapsulation. Optimization related to the pH values used is at pH 6.5 and pH 5 to maximize the positive charge of chitosan (amine group protonation) and the negative charge of alginate and pectin (carboxylate group deprotonation) (Chiesa *et al.* 2008).

The components of the polymeric nanoparticle system were selected based on the optimization that had been conducted. In summary, the ratios of SLE to chitosan (1:7, 1:5, 1:9), sodium tripolyphosphate to chitosan (1.5:1, 1:1, 2:1), chitosan to alginate (1:1, 1:2, 2:1), chitosan to pectin (1:2, 1:1, 5:1), EAFSL to chitosan (1:0.18, 1:4, 1:3), sodium tripolyphosphate to chitosan (1.5:1, 1:1, 1:1.5), chitosan to alginate (1:1.5, 1:2, 2:1), and chitosan to pectin (1.2:1, 1.3:1) can be seen in Tables 1 and 2. The best formula will be chosen based on considerations of physicochemical properties and the characterization of the SLE and EAFSL nanoparticles produced.

Table 6. Physicochemical properties of SLE and EAFSL nanoparticles

Formulas	Organoleptic properties					pH	F	% EE	% DL
	Color	Odor	Taste	Form	Consistency				
SLE nanoparticles with chitosan and alginate									
I A-E	slightly yellow	acidic	acidic	clear solution	Liquid	3.41±0.077	1	97.86	0.009
II A-E	slightly yellow	acidic	acidic	clear solution	Liquid	3.03±0.045	1	98.13	0.009
III A-E	slightly yellow	acidic	acidic	clear solution	Liquid	3.10±0.020	1	98.46	0.009
SLE nanoparticles with chitosan and pectin									
I P-E	slightly yellow	acidic	acidic	clear solution	Liquid	3.03±0.055	1	98.07	0.009
II P-E	slightly yellow	acidic	acidic	clear solution	Liquid	3.21±0.015	1	97.80	0.009
III P-E	slightly yellow	acidic	acidic	clear solution	Liquid	3.28±0.032	1	98.13	0.009
EAFSL nanoparticles with chitosan and alginate									
I A-F	slightly yellow	acidic	acidic	clear solution	Liquid	2.64±0.0152	1	98.30	0.012
II A-F	slightly yellow	acidic	acidic	clear solution	Liquid	3.04±0.020	1	98.50	0.012
III A-F	slightly yellow	acidic	acidic	clear solution	Liquid	2.58±0.0152	1	98.74	0.012
EAFSL nanoparticles with chitosan and pectin									
I P-F	slightly yellow	acidic	acidic	clear solution	Liquid	2.56±0.0251	1	98.30	0.012
II P-F	slightly yellow	acidic	acidic	clear solution	Liquid	2.55±0.0472	1	98.50	0.012
III P-F	slightly yellow	acidic	acidic	clear solution	Liquid	2.49±0.0208	1	98.90	0.012

Notes:

I A-E = SLE nanoparticles with 1% chitosan and 1% alginate
II A-E = SLE nanoparticles with 0.75% chitosan and 1.25% alginate
III A-E = SLE nanoparticles with 1.25% chitosan and 0.75% alginate
I P-E = SLE nanoparticles with 1% chitosan and 0.5% pectin
II P-E = SLE nanoparticles with 0.75% chitosan and 0.75% pectin
III P-E = SLE nanoparticles with 1.25% chitosan and 0.25% pectin
I A-F = EAFSL nanoparticles with 1% chitosan and 1.5% alginate
II A-F = EAFSL nanoparticles with 0.75% chitosan and 1.25% alginate
III A-F = EAFSL nanoparticles with 0.5% chitosan and 1% alginate
I P-F = EAFSL nanoparticles with 1% chitosan and 0.875% pectin
II P-F = EAFSL nanoparticles with 0.75% chitosan and 0.625% pectin
III P-F = EAFSL nanoparticles with 1.25% chitosan and 0.375% pectin

3.3. Characterization of the physicochemical properties of SLE and EAFSL nanoparticles

The physicochemical characterization of SLE and EAFSL nanoparticles was conducted to understand and describe

their properties, including organoleptic characteristics, pH, sedimentation degree, encapsulation efficiency, and surface morphology. The purpose of this characterization was to confirm the successful formation of nanoparticles and the encapsulation of SLE and EAFSL in the nanoparticle system.

In this study, the physicochemical characterization of various SLE and EAFSL nanoparticle formulations using natural polymers, such as chitosan, alginate, and pectin with different concentrations, is presented in the Table 6 below.

Figure 3. Formulation of SLE and EAFSL nanoparticles with chitosan and alginate polymers

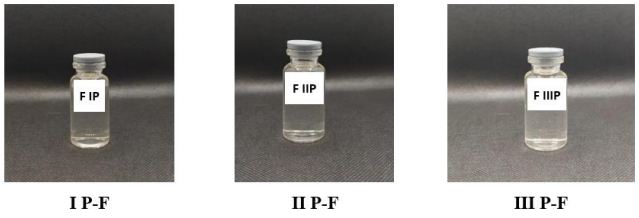

Figure 4. Formulation of SLE and EAFSL nanoparticles with chitosan and pectin polymers

In this study, Figure 3 show image of formulation of SLE and EAFSL nanoparticles with chitosan and alginate polymers, while Figure 4 show image of formulation of SLE and EAFSL nanoparticles with chitosan and pectin polymers. The physicochemical properties of SLE and EAFSL nanoparticles with chitosan-alginate and chitosan-pectin polymers exhibit a slightly yellowish color, acidic odor, acidic taste, clear solution form, and liquid consistency. The purpose of observing these organoleptic characteristics is to visually assess the sensory attributes of nanoparticles, such as color, odor, taste, form, and consistency. The acidic odor and taste are attributed to the acidic pH of SLE. The pH of SLE nanoparticles ranges from 3.03 – 3.41, while EAFSL falls within the pH range of 2.49 – 3.04. The clear solution form and liquid consistency indicate perfect solubility of the extracts in the carrier fluid. The slightly yellowish color is influenced by the dark brownish color of SLE and EAFSL. Since SLE and EAFSL dissolve completely in the carrier fluid, no precipitates or agglomerations of nanoparticles are found, resulting in a sedimentation degree value of 1.

The purpose of observing pH is to measure the acidity or alkalinity level of a solution, providing essential information related to the chemical balance and potential reactions within a system. Meanwhile, the objective of observing the sedimentation degree is to assess how quickly or slowly solid particles in a solution may settle, offering insights into the stability and consistency of a colloidal or suspension system (Waqas *et al.* 2023).

Efficiency of encapsulation and drug loading are crucial parameters in nanoparticle formulation, as they influence the effectiveness of drug delivery and the administered dosage. These parameters are closely related to the ability of nanoparticles to efficiently transport and release drugs to the desired target site. The purpose of determining the encapsulation efficiency and drug loading in this study is to understand the amount of SLE and EAFSL successfully encapsulated in the nanoparticle system. The method used for measuring encapsulation efficiency and drug loading is spectrophotometry, where measurements are conducted by assessing the sample absorbance and calculating the amount of SLE and EAFSL entrapped based on a previously established calibration curve. The encapsulation results can be seen in Figure 13 and 14. From the research results, the nanoparticle formulas SLE IA-E, IIA-E, and IIIA-E with chitosan and alginate polymers have % EE ranging from 97.86% to 98.46%, while the nanoparticle formulas EAFSL IA-F, IIA-F, and IIIA-F with chitosan and alginate polymers have % EE ranging from 98.30% to 98.74%, with each formula exhibiting high encapsulation efficiency values exceeding 80%. A high % EE is desirable as it indicates that a significant portion of SLE and EAFSL has been successfully encapsulated in the nanoparticles, enhancing the efficiency and safety of drug delivery to the desired target (Reis *et al*. 2017).

For the nanoparticle formulas SLE IP-E, IIP-E, and IIIP-E with chitosan and alginate polymers, % EE ranges from 97.80% to 98.13%, while the nanoparticle formulas EAFSL IP-F, IIP-F, and IIIP-F with chitosan and alginate polymers have % EE ranging from 98.30% to 98.90%, each formula maintaining high encapsulation efficiency values above 80%. It demonstrates that the encapsulation of EAFSL is higher than that of SLE, whether using chitosan-alginate or chitosan-pectin polymers.

Apart from that, the results of drug loading between SLE and EAFSL show no significant differences. This indicates that the surface coating of nanoparticles by alginate and pectin does not affect drug loading values. Drug loading values are not directly influenced by the polymer concentration in the formula but are influenced by the SLE and EAFSL content's impact on the total weight of the components in the nanoparticle formula due to the increased mass of the polymer.[40] In this regard, EAFSL has a larger drug loading than SLE, with % drug loading (DL) for EAFSL at 0.012% (120 ppm), while % drug loading (DL) for SLE is at 0.009% (90 ppm).

The efficiency of encapsulation and drug loading in a formula affects the effectiveness of anti-aging in drug delivery and the administered dosage. A higher % EE value implies a greater ratio of SLE and EAFSL within one particle, indicating a higher dose administered with a smaller number of nanoparticles. High drug loading values are also crucial for enhancing the formula's effectiveness in drug delivery.[41] In addition to % EE, the physicochemical properties of nanoparticles can be observed through the surface morphology of SLE and EAFSL nanoparticles, analyzed using transmission electron microscopy (TEM), as shown in the Figure 5 below.

The surface morphology of SLE nanoparticles was characterized using chitosan-alginate and chitosan-pectin polymers through transmission electron microscopy (TEM).

Transmission electron microscopy (TEM) is an advanced imaging technique utilizing an electron beam, as opposed to light, to examine the ultrastructure of materials at the nanoscale. In TEM, the sample is positioned in the path of an electron beam, and the transmitted electrons generate high-resolution images. Due to the shorter wavelength of electrons compared to visible light, TEM achieves significantly higher resolution than light microscopy. The TEM results illustrate the surface morphology structure of SLE nanoparticles using chitosan and alginate polymers, revealing a distinct and well-defined nanoparticle chain structure cross-linked by sodium tripolyphosphate chains, as depicted in the Figure 6 below.

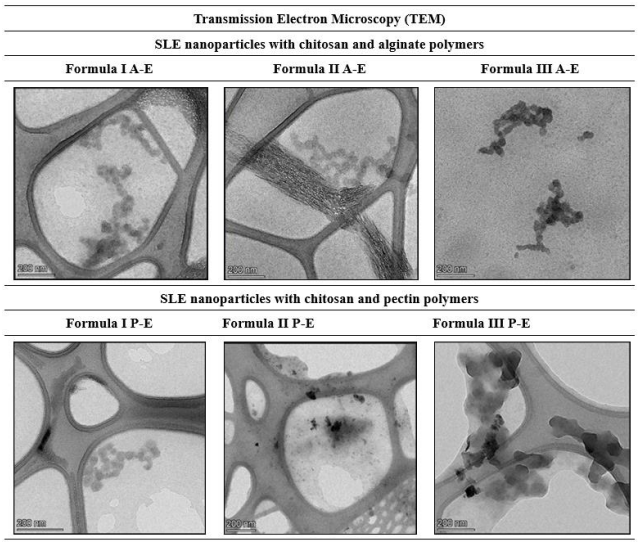

Figure 5. Surface morphology of SLE nanoparticles

Notes:

I A-E = SLE nanoparticles with 1% chitosan and 1% alginate

II A-E = SLE nanoparticles with 0.75% chitosan and 1.25% alginate

III A-E = SLE nanoparticles with 1.25% chitosan and 0.75% alginate

I P-E = SLE nanoparticles with 1% chitosan and 0.5% pectin

II P-E = SLE nanoparticles with 0.75% chitosan and 0.75% pectin

III P-E = SLE nanoparticles with 1.25% chitosan and 0.25% pectin

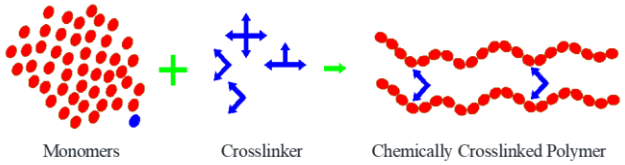

Figure 6. Surface morphology structure of nanoparticles using polymers

In SLE nanoparticles using a polymer concentration where chitosan equals the amount of pectin, and chitosan concentration is five times that of pectin, the surface morphology reveals the formation of a protective layer by pectin (enteric) on its surface. This phenomenon results in faster settling during storage, and SLE is encapsulated within the nanoparticles, making it challenging to release, thereby enhancing anti-aging activity.

The utilization of chitosan, alginate, and pectin in nanoparticle fabrication significantly impacts the resulting surface morphology. Chitosan, a positively charged polymer derived from chitin, can interact with the negative charge of nanoparticles, producing an organized surface structure (Kimberly *et al.* 2006). Alginate, derived from brown algae, imparts stability and strength to the nanoparticles, forming an even and structured layer on the surface. Meanwhile, pectin, a polysaccharide found in plant cell walls, provides mucoadhesive properties to the nanoparticles. The combination of these three elements creates a complex and controllable nanoparticle surface morphology system, opening up potential applications in drug delivery, food ingredients, and various other fields (Kimberly *et al*. 2005).

Table 7. Characterization of SLE nanoparticles with chitosan and alginate polymers

Formulas	Particle size (nm)	PI	Zeta potential (mV)	% inhibition
I A-E	173.0	1.401	-22.1	0
II A-E	189.7	1.468	-20.0	39.40
III A-E	187.6	1.382	-22.3	18.20
Parameter	50–200	0.1–10	±20–±30	30.18 (SLE)

Notes:

I A-E = SLE nanoparticles with 1% chitosan and 1% alginate

II A-E = SLE nanoparticles with 0.75% chitosan and 1.25% alginate

III A-E = SLE nanoparticles with 1.25% chitosan and 0.75% alginate

3.4. Characterization and testing of SLE and EAFSL nanoparticle activity against elastase enzyme

Particle size, polydispersity index (PI), and zeta potential are crucial for characterizing and understanding the properties of nanoparticles as a delivery system in anti-aging applications.[44] The objective of this testing is to observe the influence of the ratio of chitosan-alginate and chitosan-pectin polymers on the characterization of particle size, polydispersity index (PI), and zeta potential of nanoparticles. Particle size and polydispersity index measurements are conducted using a particle size analyzer (PSA) with the dynamic light scattering (DLS) method. DLS is a commonly used method for measuring particle size and polydispersity index in nanoparticle systems. This method assesses changes in light intensity produced or scattered by particles as they move randomly in a solution (Lazaridou *et al.* 2020).

In this study, zeta potential was measured using electrophoretic light scattering (ELC) method. This method combines the principles of electrophoresis with light

scattering measurements to estimate the zeta potential of nanoparticles (McNeil-Watson *et al.* 2013). The results of the characterization measurements of SLE nanoparticles with chitosan-alginate polymer are presented in the Table 7 below.

The table above reveals that SLE nanoparticles with the natural polymers (i.e., chitosan and alginate) exhibit the best characterization. They show the highest inhibitory activity against elastase enzyme and possess the most favorable surface morphology compared to other formulations. Specifically, formula IIA-E, with a polymer concentration of 0.75% chitosan and 1.25% alginate, stands out with a particle size of 189.7 nm, a polydispersity index of 1.468, and a zeta potential of -20.0 mV. The inhibitory value of 1.4 mg/ml of SLE nanoparticles against elastase enzyme is the highest, reaching 30.18%. The choice of characterizing SLE nanoparticles with chitosan and alginate polymer is based on the highest inhibition against elastase enzyme, observed in formula IIA-E at 39.40%, followed by formula IIIA-E at 18.20%. This is illustrated in the Figure 7 below.

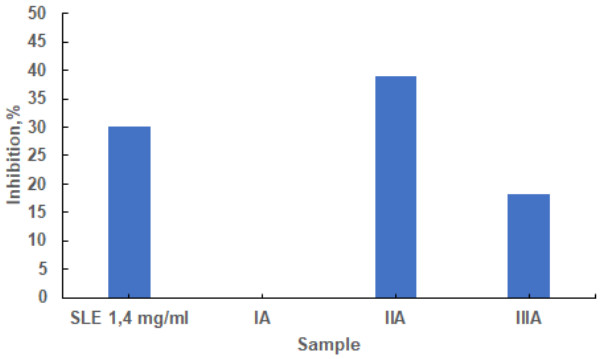

Figure 7. Comparison of elastase enzyme inhibition percentage between SLE and SLE nanoparticles with chitosan and alginate polymers

Table 8. Characterization of EAFSL nanoparticles with chitosan and alginate polymers

Formulas	Particle size (nm)	PI	Zeta potential (mV)	% inhibition
I A-F	183.0	1.781	-20.4	-
II A-F	205.0	1.975	-11.3	87.30
III A-F	172.9	1.828	-15.0	-
Parameter	50–200	0.1–1.0	±20–±30	22.42 (EAFSL)

Notes:

I A-F = EAFSL nanoparticles with 1% chitosan and 1.5% alginate

II A-F = EAFSL nanoparticles with 0.75% chitosan and 1.25% alginate

III A-F = EAFSL nanoparticles with 0.5% chitosan and 1% alginate

Table 9. Characterization of SLE nanoparticles with chitosan and pectin polymers

Formulas	Particle size (nm)	PI	Zeta potential (mV)	% inhibition
I P-E	200.3	1.984	-23.6	27.28
II P-E	200.7	1.672	-22.4	12.14
III P-E	193.4	1.478	-27.9	-3.02
Parameter	50–200	0.1–1.0	±20–±30	30.18 (SLE)

Notes:

I P-E = SLE nanoparticles with 1% chitosan and 0.5% pectin

II P-E = SLE nanoparticles with 0.75% chitosan and 0.75% pectin

III P-E = SLE nanoparticles with 1.25% chitosan and 0.25% pectin

Table 10. Characterization of EAFSL nanoparticles with chitosan and pectin polymers

Formulas	Particle size (nm)	PI	Zeta potential (mV)
I P-F	175.5	1.713	-21.7
II P-F	175.3	1.887	-23.2
III P-F	176.1	1.938	-20.9
Parameter	50–200	0.1–1.0	±20–±30

Notes:

I P-F = EAFSL nanoparticles with 1% chitosan and 0.875% pectin

II P-F = EAFSL nanoparticles with 0.75% chitosan and 0.625% pectin

III P-F = EAFSL nanoparticles with 1.25% chitosan and 0.375% pectin

From the bar graph above, it can be concluded that formula IIA-E of SLE nanoparticles (with twice the concentration of alginate compared to chitosan) has a greater inhibitory effect against the elastase enzyme compared to SLE alone. Formula IA-E (SLE nanoparticles with 1% chitosan and 1% alginate) exhibit 0% inhibition. This can be attributed to two possibilities. Firstly, the polymer strongly binds with SLE, preventing its release, and secondly, the SLE nanoparticles are already dissolved in the water solvent, resulting in no anti-aging activity.

The particle size in this study falls within the range of 100-200 nm, meeting the criteria for expected nanoparticle sizes, which typically range from 50 to 200 nm (Naito *et al.* 2018). A drug compound demonstrates favorable characteristics when it is in the nanometer size range, enhancing dissolution rate, drug penetration, and

bioavailability. This, in turn, prolongs the drug's duration in systemic circulation and reduces the drug's excretion rate, resulting in a more extended and effective impact (Tamarov *et al*. 2008).

Regarding the zeta potential values, as indicated by the obtained results, it is evident that the surface coating of nanoparticles with alginate and pectin leads to a surface charge inversion. This occurs due to the charged properties of alginate and pectin, as well as the electrostatic interactions between alginate and chitosan, and pectin and chitosan. Alginate is an anionic polysaccharide with negative charges on carboxylate groups (COO^-), while chitosan is a cationic polysaccharide with positive charges on amine groups (NH_3^+). When alginate and pectin are applied to the surface of chitosan nanoparticles, the carboxylate groups on alginate and pectin interact with the amine groups on chitosan through ionic bonding or electrostatic interactions. This leads to the transfer of negative charges from alginate and pectin to the particle surface, resulting in negative zeta potential values. Additionally, since the molecules of alginate and pectin are primarily located in the outermost layer of the nanoparticles (enteric), the interaction between the negative charges of alginate and pectin and the positive charges of chitosan can induce strong electrostatic repulsion, yielding negative zeta potential values. Negative zeta potential in nanoparticles can lead to strong electrostatic repulsion. This prevents particle aggregation in a solution or biological media. The high dispersal stability of nanoparticles allows nanoparticles to stay separate from each other, maintaining the desired particle size and properties. This is crucial in drug delivery, as aggregated particles can reduce the efficiency of drug delivery to skin tissues. Nanoparticles with a negatively charged zeta potential tend to avoid adhesion to cellular surfaces or other biological components, enhancing stability, circulation in the body, and selective and efficient encapsulation, especially when coated with targeting ligands (Nokhodi *et al*. 2022; Wang *et al*. 2020).

The results of the characterization measurements of EAFSL nanoparticles with chitosan-alginate polymer are presented in the Table 8 below.

From the table above, it is evident that EAFSL nanoparticles with natural polymers (i.e., chitosan and alginate) exhibit the best characterization. Among the various formulas, F IIA-F, with a polymer concentration of 0.75% chitosan and 1.25% alginate, shows the highest inhibitory activity against elastase enzyme. The particle size is 205.0 nm, the polydispersity index is 1.975, and the zeta potential is -11.3 mV. The highest inhibitory value of EAFSL against elastase enzyme is recorded at 22.42%. The selection of characterization for EAFSL nanoparticles with chitosan and alginate polymers is based on achieving the highest inhibition against elastase enzyme, notably in F IIA-F, which reaches 87.30%, as depicted in the Figure 8 below.

The graph above indicates that the formula IIA-F of EAFSL nanoparticles with chitosan and alginate polymers has an inhibitory effect on elastase enzyme 3.6 times higher than the ethyl acetate fraction with a concentration of 1.8 mg/ml. Regarding the influence of natural polymers on the inhibitory value against the elastase enzyme, the smaller the chitosan concentration is and the larger the alginate concentration is, the higher the percentage of inhibitory value against the elastase enzyme will be. This is because chitosan, alginates, and pectin play a crucial role in modulating the inhibitory activity against the elastase enzyme. Chitosan, being a positive polymer, can interact with the elastase enzyme electrostatically, forming complexes that inhibit the enzyme's activity. Alginate, known for its ability to form a hydrogel, shields against the elastase enzyme and reduces its access to the substrate. Therefore, the use of chitosan and pectin influences the inhibitory activity against the elastase enzyme. The combined effects of chitosan and alginate create a synergistic inhibition system against elastase, demonstrating potential applications in the development of anti-aging therapy for human skin care (Kimberly *et al*. 2006; Kimberly *et al.* 2005).

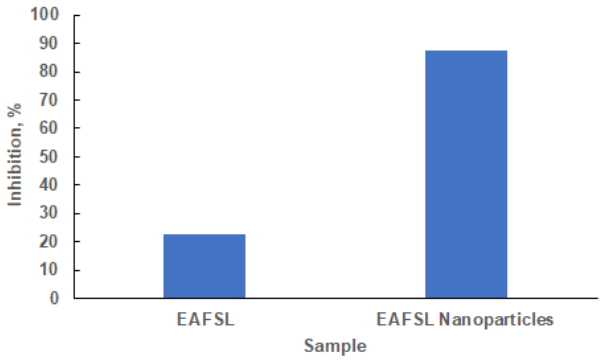

Figure 8. Comparison of elastase enzyme inhibition percentage between EAFSL and EAFSL nanoparticles with chitosan and alginate polymers

The zeta potential of EAFSL nanoparticles with chitosan and alginate polymers ranges from -11.3 mV to -20.4 mV. Thus, it may form larger aggregates due to their nanoparticle form. It is expected that in the nano-hydrogel preparation, the zeta potential will stabilize within the nano-hydrogel structure, as the hydrogel's inherent property is to encapsulate formed nanoparticles. This encapsulation will integrate the nanoparticles into the nano-hydrogel structure.

The results of the characterization measurements of SLE nanoparticles with chitosan-pectin polymer are presented in the Table 9 below.

From the table above, it can be observed that SLE nanoparticles with natural polymers (i.e., chitosan and pectin) exhibit the most favorable characteristics. Among the various formulations, F IP-E stands out with a chitosan concentration of 1% and a pectin concentration of 0.5%. This formulation demonstrates a particle size of 200.3 nm, a polydispersity index of 1.984, and a zeta potential of -23.6 mV. Additionally, it displays the highest inhibition value against elastase enzyme, reaching 30.18% at an SLE concentration of 1.4 mg/ml. The selection of this formulation for the characterization of SLE nanoparticles with chitosan and pectin polymers is based on its superior

inhibitory activity against the elastase enzyme, registering at 27.28%, compared to other formulations. This is further depicted in the Figure 9 below.

From the graph above, it is evident that all formulations of SLE nanoparticles with chitosan and pectin polymers exhibit minimal inhibitory activity against the elastase enzyme. This observation can be attributed to the morphology of the nanoparticles, as revealed by TEM results, where a pectin membrane layer acts as an enteric coating around SLE nanoparticles. This coating makes it challenging for the active substance to exit, leading to inhibited activity.

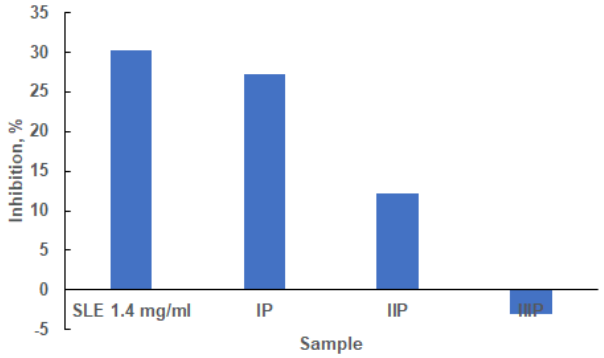

Figure 9. Comparison of elastase enzyme inhibition percentage between SLE and SLE nanoparticles with chitosan and pectin polymers

Pectin, with its mucoadhesive properties, can retain elastase enzymes on the surface, hindering their interaction with substrates. The combined effects of chitosan, alginate, and pectin create a synergistic inhibition system against elastase, showcasing potential applications in developing anti-inflammatory therapies and treatments for conditions related to elastic tissue damage in humans (Weng *et al.* 2022).

Based on the results of the obtained polydispersity index, almost all formulations fall within the range of 1.3 to 1.9. This indicates that the majority of particles are highly polydisperse, as the polydispersity index values exceed > 0.7, signifying a very wide distribution of particle sizes (non-uniform) and a likelihood of sedimentation, making them unstable. Nanoparticles with a uniform size distribution tend to be more stable in a solution medium. This reduces the possibility of particle aggregation or clumping, which can affect the properties and performance of nanoparticles. In drug delivery applications, a uniform particle size distribution can impact the efficiency of delivering the desired drug to the target. Particles with a uniform size have a better chance of penetrating tissues or overcoming biological barriers, thereby enhancing drug delivery efficiency (Wathoni *et al.* 2019).

The results of the characterization measurements of EAFSL nanoparticles with chitosan-pectin polymer are presented in the Table 10 below.

Table 11. Short-term stability of SLE and EAFSL nanoparticles

Formulas	Particle size (nm)	PI	Zeta potential (mV)	% EE	pH	Sedimentation degree
SLE nanoparticles						
I A-E	185.6	1.122	-21.6	93.82	3.30±0.037	1
II A-E	180.8	1.479	-19.2	94.06	2.63±0.01	1
III A-E	193.5	1.650	-18.0	93.52	2.67±0.01	0.2
I P-E	193.3	1.470	-22.2	93.52	2.58±0.045	1
II P-E	207.7	1.843	-23.0	95.68	2.69±0.005	0.1
III P-E	191.8	1.516	-20.1	93.82	2.67±0.015	0.07
EAFSL nanoparticles						
IA-F	183.0	1.781	-20.4	96.62	2.65±0.005	0.01
IIA-F	205.0	1.975	-11.3	96.50	2.57±0.025	1
IIIA-F	172.9	1.828	-15.0	97.26	2.59±0.01	1
IP-F	175.5	1.713	-21.7	96.10	2.61±0.01	1
IIP-F	175.3	1.887	-23.2	96.82	2.61±0.0152	0.2
IIIP-F	176.1	1.938	-20.9	97.54	2.52±0.01	0.01

Notes:

I A-E = SLE nanoparticles with 1% chitosan and 1% alginate

II A-E = SLE nanoparticles with 0.75% chitosan and 1.25% alginate

III A-E = SLE nanoparticles with 1.25% chitosan and 0.75% alginate

I P-E = SLE nanoparticles with 1% chitosan and 0.5% pectin

II P-E = SLE nanoparticles with 0.75% chitosan and 0.75% pectin

III P-E = SLE nanoparticles with 1.25% chitosan and 0.25% pectin

I A-F = EAFSL nanoparticles with 1% chitosan and 1.5% alginate

II A-F = EAFSL nanoparticles with 0.75% chitosan and 1.25% alginate

III A-F = EAFSL nanoparticles with 0.5% chitosan and 1% alginate

I P-F = EAFSL nanoparticles with 1% chitosan and 0.875% pectin

II P-F = EAFSL nanoparticles with 0.75% chitosan and 0.625% pectin

III P-F = EAFSL nanoparticles with 1.25% chitosan and 0.375% pectin

The table above reveals that EAFSL nanoparticles containing natural polymers (i.e., chitosan and pectin) exhibit superior characteristics compared to other formulations, particularly F IP-F. This specific formulation, with a concentration of 1% chitosan and 0.875% pectin, stands out with a particle size of 175.5 nm, a polydispersity index of 1.713, and a zeta potential of -21.7 mV. The size of particles plays a pivotal role in drug delivery systems through the skin. Nano-sized particles are crucial for enhancing drug activity and penetration into skin tissues. In this context, the minute size of nanoparticles in nanometers facilitates more effective penetration into deeper layers of the skin. Nanoparticles with sizes in the nanometer range can traverse intercellular gaps and overcome structural barriers in skin tissues, such as the stratum corneum layer. Furthermore, the diminutive size of nanoparticles can improve drug solubility and facilitate absorption through the skin surface. Consequently, the incorporation of nanoparticles in topical drug formulations has the potential to enhance drug delivery efficiency, optimize drug penetration into skin tissues, improve the efficacy of topical therapy, and mitigate systemic impacts (Ullah *et al*. 2022).

Table 12. pH stability of SLE nanoparticles with chitosan-alginate polymer and chitosan-pectin polymer

Formulas	0 day	1 day	7 days	14 days	21 days	28 days	2 months
I A-E	3.41±0.077	3.41±0.077	3.61±0.090	3.80±0.136	3.26±0.01	3.26±0.01	3.30±0.037
II A-E	3.03±0.045	3.03±0.045	3.21±0.037	3.19±0.030	2.67±0.045	2.67±0.045	2.63±0.01
III A-E	3.10±0.020	3.10±0.020	3.20±0.010	3.20±0.020	2.73±0.015	2.73±0.015	2.67±0.01
I P-E	3.03±0.055	3.03±0.055	3.12±0.036	3.15±0.011	2.58±0.017	2.58±0.017	2.58±0.045
II P-E	3.21±0.015	3.21±0.015	3.28±0.032	3.34±0.049	2.72±0.010	2.72±0.010	2.69±0.005
III P-E	3.28±0.032	3.28±0.032	3.25±0.060	3.26±0.036	2.67±0.015	2.67±0.015	2.67±0.015

Notes :
I A-E = SLE nanoparticles with 1% chitosan and 1% alginate
II A-E = SLE nanoparticles with 0.75% chitosan and 1.25% alginate
III A-E = SLE nanoparticles with 1.25% chitosan and 0.75% alginate
I P-E = SLE nanoparticles with 1% chitosan and 0.5% pectin
II P-E = SLE nanoparticles with 0.75% chitosan and 0.75% pectin
III P-E = SLE nanoparticles with 1.25% chitosan and 0.25% pectin

The utilization of chitosan, alginate, and pectin in nanoparticle formulations has a significant impact on particle size, polydispersity index, and zeta potential. Chitosan, acting as a positively charged polymer, contributes to the reduction of particle size through robust electrostatic interactions with the negative charge on nanoparticles. Alginate imparts stability and diminishes particle polydispersity, yielding a more homogeneous size distribution. Meanwhile, pectin can influence zeta potential by introducing surface charges that modulate interactions among particles. The synergy of these three components yields nanoparticles with the desired size, a narrow size distribution, and adjustable surface charge properties, providing enhanced control (Nunes *et al.* 2022; Muhaimin *et al.* 2023)

3.5. Short-term stability test at room temperature for 2 months

The purpose of the short-term stability test at room temperature over two months is to assess how well a product or substance can maintain its quality under typical storage conditions. This test is conducted to ensure that the product or substance does not undergo significant physical, chemical, or microbiological changes during a relatively brief storage period. By conducting short-term stability testing, we can identify potential issues or product degradation early on, providing an opportunity for improvement or formulation modifications if necessary. The ultimate goal is to ensure that the product or substance continues to meet the desired quality standards set by the manufacturer and can deliver the expected safety and efficacy to consumers. This short-term stability test also aids in developing storage guidelines and product handling information that can assist relevant stakeholders (Zhu *et al.* 2024).

The short-term stability of SLE and EAFSL nanoparticles with chitosan-alginate and chitosan-pectin polymers after a two-month room temperature storage period can be observed in the Table 11 below.

Short-term stability testing during two months of room temperature storage involves a series of procedures to ensure that a specific product or substance remains consistent and undergoes no significant changes during this storage period. Firstly, it is ensured that the storage environment meets the specified room temperature requirements. Following that, representative samples of the product or substance are taken, and their physical, chemical, and microbiological properties are observed at predetermined intervals. The analysis of these observations includes critical parameters that can influence the quality and safety of the product. If there are no significant changes in these parameters over two months, it is considered that the product or substance remains stable during room temperature storage. This short-term stability testing process is crucial to ensure that the product or substance continues to meet the expected quality standards throughout its shelf life.[38] The pH stability graph of SLE nanoparticles with chitosan-alginate and chitosan-pectin polymers during two-month storage at room temperature is presented in Figure 10 (a and b) below.

Nanoparticles with positively charged polymers, such as chitosan, tend to be more stable at low pH (acidic), while nanoparticles with negatively charged polymers, like alginate and pectin, are more stable at high pH (alkaline). The pH stability of SLE nanoparticles with chitosan polymer tends to increase during storage at low pH. Chitosan possesses weak acidic properties, indicating a positive charge at low pH. Therefore, nanoparticles made with chitosan carry a positive charge at low pH, preventing aggregation or clumping of positively charged nanoparticles and enhancing stability (Stetefeld *et al.* 2016).

Table 13. Sedimentation degree stability of SLE nanoparticles with chitosan alginate polymer and chitosan pectin polymer.

Formulas	0 day	1 day	7 days	14 days	21 days	28 days	2 months
I A-E	1±0	1±0	1±0	1±0	1±0	1±0	1±0
II A-E	1±0	1±0	1±0	1±0	1±0	1±0	1±0
III A-E	1±0	1±0	1±0	1±0	1±0	1±0	0,2±0
I P-E	1±0	1±0	1±0	1±0	1±0	1±0	0,1±0
II P-E	1±0	1±0	1±0	1±0	1±0	1±0	0,1±0
III P-E	1±0	1±0	1±0	1±0	1±0	1±0	0,07±0

Notes :
I A-E = SLE nanoparticles with 1% chitosan and 1% alginate
II A-E = SLE nanoparticles with 0.75% chitosan and 1.25% alginate
III A-E = SLE nanoparticles with 1.25% chitosan and 0.75% alginate
I P-E = SLE nanoparticles with 1% chitosan and 0.5% pectin
II P-E = SLE nanoparticles with 0.75% chitosan and 0.75% pectin
III P-E = SLE nanoparticles with 1.25% chitosan and 0.25% pectin

Table 14. Stability % EE of SLE nanoparticles with chitosan alginate polymer and chitosan pectin polymer

Formulas	0 day	1 day	7 days	14 days	21 days	28 days	2 months
I A-E	90.58	90.58	93.16	94.72	94.72	93.82	93.82
II A-E	94.48	94.48	94.06	93.82	93.82	94.06	94.06
III A-E	98.08	98.08	94.06	93.40	93.40	93.52	93.52
I P-E	94.60	94.60	93.82	93.04	93.04	93.52	93.52
II P -E	95.50	95.50	95.92	95.02	95.02	95.68	95.68
III P-E	94.48	94.48	93.94	93.82	93.82	93.82	93.82

Notes:
I A-E = SLE nanoparticles with 1% chitosan and 1% alginate
II A-E = SLE nanoparticles with 0.75% chitosan and 1.25% alginate
III A-E = SLE nanoparticles with 1.25% chitosan and 0.75% alginate
I P-E = SLE nanoparticles with 1% chitosan and 0.5% pectin
II P-E = SLE nanoparticles with 0.75% chitosan and 0.75% pectin
III P-E = SLE nanoparticles with 1.25% chitosan and 0.25% pectin

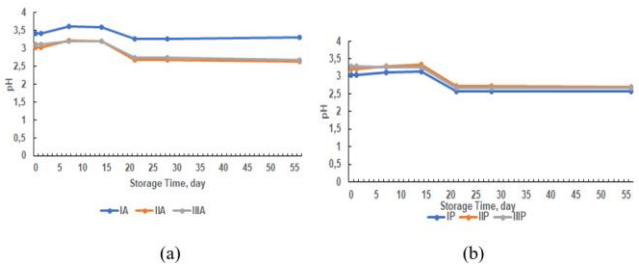

(a) (b)

Figure 10. pH stability of SLE nanoparticles with chitosan-alginate polymer (a) and chitosan-pectin polymer (b).

According to Stokes' law, stability can also be observed from the sedimentation degree value which can be calculated by observing the speed of particles in nanoparticle size when settling under the influence of gravity during storage. Particle size and particle density, medium viscosity and the difference in density between particles and the medium are some of the factors that affect the sedimentation degree. Measurements can be made directly by recording how long it takes for particles to reach the bottom of the container or indirectly by using the turbidimetry method to measure the turbidity of the solution over time. The sedimentation degree (F) can be obtained through theoretical calculations using the sedimentation equation and particle characteristic data. A good sedimentation degree is one that does not experience sedimentation during storage with a value of F = 1, while F <1 nanoparticles experience sedimentation and stability during storage is not good (Sun *et al.* 2023).

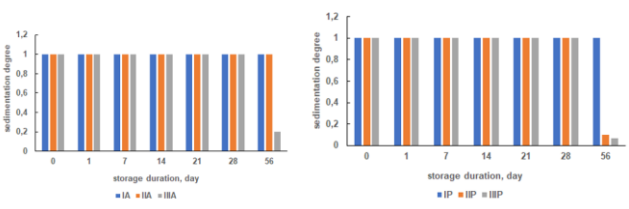

(a) (b)

Figure 11. Sedimentation degree stability of SLE nanoparticles with chitosan-alginate polymer (a) and chitosan-pectin polymer (b)

The sedimentation degree stability graph of SLE nanoparticles with chitosan-alginate and chitosan-pectin

polymers during two-month storage at room temperature is presented in Figure 11 below. While, Table 13 inform about sedimentation degree stability of SLE nanoparticles with chitosan alginate polymer and chitosan pectin polymer.

The graph in Figure 11a above shows the impact of chitosan and alginate polymers on the characterization and stability of SLE nanoparticles. As the concentration of chitosan decreases and the concentration of alginate increases, the characterization improves, and the nanoparticles become more stable, showing no signs of precipitation. Conversely, with an increase in chitosan concentration and a decrease in alginate concentration, the stability decreases, and precipitation occurs during storage. Among the SLE nanoparticle formulations with chitosan and alginate polymers, formulas IA and II A prove to be stable during a two-month storage period at room temperature.

The graph in Figure 11b above presents the influence of chitosan and pectin polymers on the characterization and stability of SLE nanoparticles. When the concentration of chitosan is twice that of pectin, both the characterization and stability improve. However, when the concentrations of chitosan and pectin are equal, and the concentration of chitosan is five times that of pectin, the formation of a pectin coating (enteric) occurs on its surface, leading to faster precipitation during storage. Among the SLE nanoparticle formulations with chitosan and pectin polymers, formula I P proves to be stable during a two-month storage period at room temperature.

Furthermore, the stability of % EE in SLE nanoparticle formula IIA-E with chitosan and alginate polymers maintains a stable % EE from initial production until the two-month storage at room temperature (Figure 12 a dan 12 b). In other words, the use of chitosan and alginate polymers does not affect % EE during storage. Meanwhile, Table 14 inform about stability % EE of SLE nanoparticles with chitosan alginate polymer and chitosan pectin polymer.

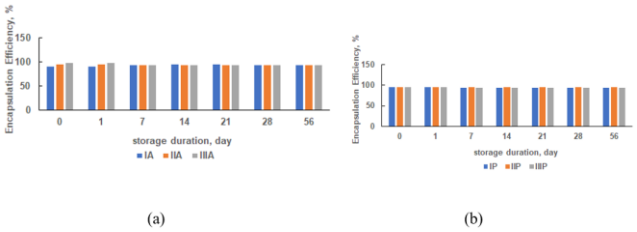

Figure 12. Stability of % EE of SLE nanoparticles with chitosan-alginate (a) and polymer chitosan-pectin polymer (b)

The stability of % EE in SLE nanoparticle formula IP-E with chitosan and pectin polymers remains consistent from the initial production to the two-month storage at room temperature. The use of chitosan and pectin polymers does not impact % EE during storage. Similarly, the utilization of chitosan, alginate, and pectin polymers does not affect % EE during storage, not only in formula IP-E but also in almost all formulations, maintaining stable % EE throughout the storage period.

4. Conclusions

From the above research results, it can be concluded that the types and concentrations of natural polymers (i.e., chitosan, alginate, and pectin) in the production of SLE and EAFSL nanoparticles significantly influence the characterization, surface morphology, stability, and activity of nanoparticles against the elastase enzyme. The best SLE and EAFSL nanoparticles with chitosan and alginate polymers are formulas IIA-E and IIA-F, while the best SLE and EAFSL nanoparticles with chitosan and pectin polymers are formulas IP-E and IP-F. The SLE and EAFSL nanoparticles that exhibit the highest elastase enzyme inhibition activity are those with chitosan and alginate polymers compared to those with chitosan and pectin polymers. This is because the SLE and EAFSL nanoparticles with chitosan and pectin polymers are coated with a strong membrane or layer of pectin polymer on the surface, making it difficult for SLE and EAFSL to be released from the nanoparticles and inhibit the elastase enzyme.

Author contributions

Conceptualization: M.M, A.Y.C & W.S.; Methodology: U.L., M.M., A.Y.C & W.S; Data curation: U.L; M.M, W.S & A.Y.C; Writing—Original Draft Preparation: U.L.; Writing—Review and Editing: M.M, A.Y.C & W.S; Supervision: M.M., A.Y.C., & W.S.; Funding Ac-quisition: M.M, A.Y.C & W.S; All authors have read and approved the final manuscript.

Availability of data and materials

The datasets used and/or analysed during the current study available from the corresponding author on reasonable request

Conflict of interest

The authors declare no conflict of interest.

Acknowledgment

We acknowledge the Ministry of Education, Culture, Research, and Technology of the Republic of Indonesia as a Doctoral Dissertation Grant in 2024.

References

Afzal O., Rizwanullah M., Atamimi A., Alossaimi M., Kamal M., Ahmad J. (2023). Harnessing natural polysaccharides-based nanoparticles for oral delivery of phytochemicals: Knocking down the barriers. *Journal of Drug Delivery Science and Technology*. 82, 104368.

Arozal W., Louisa M., Rahmat D., Chendrana P., Shandhiutami. N.M.D. (2021). Development, Characterization and Pharmacokinetic Profile of Chitosan-Sodium Tripolyphosphate Nanoparticle Based Drug Delevery System for Curcumin. *Advanced Pharmaceutical Bulletin*. 11, 1, 77–85.

Amin H., Osman. S.K., Mohammed A.M., Zayed G. (2023). Gefinitib-loaded Starch Nanoparticles for Battling Lung Cancer: Optimazation by Full Factorial Design and In vitro Cytotoxity Evaluation. *Saudi Pharmaceutical Journal*. 31, 1, 29–54.

Arvaniti E.C., Juenger M.C.G., Bernal S.A., Duchesne J., Courard L., Leroy S., Provis. J.L., Klemm A., De Belie N. (2015).

Determination of Particel Size, Suraface Area and Shape of Supplementary Cementtious Materials by Different Techniques. *Materials and Structures*. 48, 1, 3687–3701.

Balde A., Benjakul S., Kim Se-Kwon., Nazeer R. (2023). Development and in vitro effects of thiolated chitosan nanoparticles for the sustained delivery of inflammation suppressing bioactive peptide. *Journal of Drug Delivery Science and Technology*. 88, 104971.

Cahyani L.D. (2018). Fractionation of Antituberculosis Compounds from N-Hexane Soluble Extract of Red Teak Leaves (Tectona grandis L F). Universitas Negeri Alauddin Makasar.

Chiesa E., Dorati R., Conti B., Modena T., Cova E., Meloni F., Genta I. (2008). Hyaluronic Acid-Decorated Chitosan Nanoparticle for CD44-targeted Delevery of Everolimus. *International Journal of Molecular Sciences*. 19, 8.

Cai K., He X., Song Z., Yin Q., Zhang Y., Uckun F.M., Jiang C., Cheng J. (2015). Dimeric Drug Polymeric Nnaoparticles With Exceptionally High Drug Loading and Quantitative Loading Efficiency. *Journal of The American Chemical Society*. 137, 10, 3458–3461.

Deniz. (2019). Synthesis of Aloe Vera Loaded Chitosan Nanoparticle with Ionic Gelling Method. *Scientific Meeting on Electrical-Electronics and Biomedical Engineering and Computer Science*. EBBT 87420772019.

Desu P., Lanka H., Tippeswamy L., Reddy.V.A., Keshava. D.P., Soujanya J., Satya. B.L., Anusha R. (2022). Formulation and Evaluation of Fluvastatib-loaded Nanoparticles by Nanoprecepitration Method. *International Journal of Drug Delivery Technology*. 12, Issue 3, 1166–1170.

Desmiaty Y., Saputri. F.C., Hanafi M., Prastiwi R., Elya B. (2020). Anti-Elastase, Anti-Tyrosinase, And Anti-Oxidant of Rubus Fraxinifolius Stem Methanolic Extract. *Pharmacogn Journal*. 12, 2, 271–275.

Gul M., Khan R.S., Islam Z., Khan S., Shumaila A., Umar S., Khan S., Brekhna., Zahoor M., Ditta A. (2024). Nanoparticles in plant resistance against bacterial pathogens: current status and future prospects. *Molecular Biology Reports*. 51, Issue 1, 92.

Javid N.K., Dounighi N.M., Bidgol S.H. (2024). Entrapment of Digoxin-KLH Conjugate in Alginate/Chitosan Nanoparticles: A New Antigen Delivery System For Production of Anti-digoxin Antibodies. *Pharmaceutical Nanotechnology*. 2, Issue 1, 68–78.

Jiang X., Yu Y., Ma S., Li L., Yu M., Han M., Yuan Z., Zhang J. (2024). Chitosan nanoparticles loaded with Eucommia ulmoides seed essential oil: Preparation, characterization, antioxidant and antibacterial properties. *International Journal of Biological Macromolecules*. 257, 128820.

Kurl S., Kumar A., Reena., Mittal N., Singh D., Bassi P., Kaur G. (2023). Challenges, opportunities, and future prospects of polysaccharide-based nanoparticles for colon targeting: A comprehensive review. *Carbohydrate Polymer Technologies and Applications*. 6, 100361.

Kumar D., Singh R., Gautam M. (2024). Impact of surfactant-assisted synthesis on the structural, optical, and dielectric characteristics of ZnO nanoparticles. Nano Express. 5, Issue 11, 015002.

Kalam M.A. (2016). Development of Chitosan Nanoparticle Coated With Hyaluronic Acid For Topical Ocular Delevery of Dexamethansone. *International Journal of Biological Macromolecules*. 9, 127–136.

Kimberly L., Douglas., Ciriaco A.P., Maryam T. (2006). Effects of alginate inclusion on the vector properties of chitosan-based nanoparticles. *Journal of Controlled Release*. 115, 354–366.

Kimberly L., Douglas., Maryam T. (2005). Effect of experimental parameters on the formation of alginate–chitosan nanoparticles and evaluation of their potential application as DNA carrier. *Journal of Biomaterials Science, Polymer Edition* 16, 1, 43–56.

Lazaridou M., Christodoulou E., Nerantzaki M., Kostoglou M., Lambropoulou D.A., Katsarou A., Pantopoulos K., Bikiaris D.N. (2020). Formulation and In Vitro Characterization of Chitosan Nanoparticles Loaded With The Iron Chelator Deferoxamine Mesylate (DFO). *Pharmaceutics* 12, 3, 12030238.

Lestari U., Muhaimin M., Chaerunisaa A.Y., Sujarwo W. (2023a). Improved Solubility and Activity of Natural Product in Nanohydrogel. *Pharmaceuticals*. 16, 701.

Lestari U., Muhaimin M., Chaerunisaa A.Y., Sujarwo W. (2023b). Anti-aging potential of plants of the Anak dalam tribe, Jambi, Indonesia. *Pharmaceuticals*. 16, 9, 103390.

Lestari U., Muhaimin M., Chaerunisaa A.Y., Sujarwo W. (2023c). Antioxidant Activities and Phytochemical Screening of Ethanol Extract From Surian Leaves (Toona sinensis). *International Journal of Applied Pharmaceutics*. 15 , Suppl 2, 37–43.

Lestari U., Yuliawati Y., Sani F., Yuliana Y., Muhaimin M. (2023d). Antioxidant Activities of Scrub Body Lotion Extract of Surian Leaves (Toona sinensis) With Powder Scrub Date Seeds (Phoenix dactylifera). Indones. *Journal of Pharmaceutical Science and Technology* 1, Suppl 1, 60–69.

Milenkova S., Ambrus R., Mukhtar M., Pilicheva B., Marudova M (2024). Spray-Dried Chitosan Hydrogel Particles as a Potential Delivery System for Benzydamine Hydrochloride, Gels 10, Suppl 3,189.

Meng Y., Qiu C., Li, X.; McClements, D.; Shang, S.; Jiao, A.; Jin, Z. (2024). Polysaccharide-based nano-delivery systems for encapsulation, delivery, and pH-responsive release of bioactive ingredients. *Critical Reviews in Food Science and Nutrition*. 64, Issue 1, 187–201.

Medha and Sethi, S. (2024). Chitosan based hybrid superabsorbent for controlled drug delivery application. *Biotechnology Progress*.

Mondal A., Nayak A.K., Chakraborty P., Baneerje S., Nandy B.C. (2023). Natural Polymeric Nanobiocomposites for Anti-Cancer Drug Delivery Therapeutics: A Recent Update. Pharmaceutics. 15, Issue 8, 2064.

Magdassi S. (1997). Delivery systems in cosmetics. *Colloids and Surfaces A: Physicochemical and Engineering Aspects*. 123–124.

Muhaimin M., Chaerunisaa A.Y., Bodmeier R. (2023). Preparation and evaluation of various formulation effects of the second emulsion on the shape and release profile of propranolol HCl from ethyl cellulose microparticle blends. *Polymer International*. 72, 3, 383–39.

McNeil-Watson F. (2013). Electrophoretic Light Scattering. In Encyclopedia of Biophysics. *Springer Berlin Heidelberg*. 648–654.

Nunes D., Andrade S., Ramalho M.J., Loureiro J.A., Pereira M.C. (2022). Polymeric Nanoparticles Loaded Hydrogels for Biomedical Applications : A Systematic Review on In Vivo Findings. *Polymers*. 14, 5, 1–28.

Naito M., Yokoyama T., Hoskawa K., Nogi K. (2018). *Nanoparticle Technology Handbook*. Elsivier.

Nokhodi F., Nekoei M., Gooddarzi M.T. (2022). Hyaluronic Acid Coated Chitosan Nanoparticles as Targeted Carrier of

Tamoxifen Against MCF7 and TMX resistant MCF7 Cells. *Journal of Material Sciences: Materials in Medicine*. 33, 2.

Pires-Patricia C., Mascarenhas M.P., Pedrosa K., Lopes D., Lopes J., Macario-Soares A., Peixoto D., Giram P., Veiga F., Paiva-santos A. (2023). Polymer-based biomaterials for pharmaceutical and biomedical applications: A focus on topical drug administration. *European Polymer Journal*. 1873, 111868.

Patravale V.B., Mandawgade S.D. (2008). Novel cosmetic delivery systems: An application update. *In International Journal of Cosmetic Science*. 30, 1.

Qureshi M.A., Khatoon F. (2019). Different types of smart nanogel for targeted delivery. *Journal of Science: Advanced Materials and Devices*. 4, 201–212.

Rani E and Radha G. (2023). Investigation of In Vivo Bioavailability Enhancement of Iloperidone-Loaded Solid Self-Nanoemulsifying Drug Delivery Systems: Formulation and Optimization Using Box-Behnken Design and Desirability Function. *Journal of Pharmaceutical Innovation*. 18, Issue 3, 1030–1046.

Reis C.P., Neufeld R.J., Veiga F. (2017). Preparation of Drug Loaded Polymeric Nanoparticles. *In Nanomedicine in Cancer*. 197-240.

Sharma S., Kanugo A., Kaur T., Choudhary D. (2023). Formulation and Characterization of Self-Microemulsifying Drug Delivery System (SMEDDS) of Sertraline Hydrochloride. *Recent Patents on Nanotechnology*. 18, Issue 1, 3–16.

Sindhu R.K., Gupta R., Wadhera G., Kumar P. (2022). Modern Herbal Nanogels: Formulation, Delivery Methods, and Applications. *Gels*. 8, 2, 1–23.

Stetefeld J., McKenna S.A., Pate T.R. (2016). Dynamic Light Scattering: a Parctical Guide and Applications in Biomedical Sciences. *Biophysical Reviews*. 8, 4, 409–427.

Sun L., Wu J., Chen M., Wang T., Shang Z., Liu J., Huang M., Wu P..(2023). Interaction of polystyrene nanoplastics with impurity-bearing ferrihydrite and implication on complex particle sedimentation. *Science of The Total Environment* 901.

Taslim T., Pratama R.H. (2020). Analysis Of The Antioxidant Power Of Secondary Metabolite Compounds Of Surain Leaf Ethanol Extract (Toona sinensis(Juss) M.Roem). *J Akad Farm Pray*. 5, 2, 19–28.

Tian B., Qiao X., Guo S., Li A., Xu Y., Cha J., Zhang X., Ma D.(2024). Synthesis of β-acids loaded chitosan-sodium tripolyphosphate nanoparticle towards controlled release, antibacterial and anticancer activity. *International Journal of Biological Macromolecules*. 257, 128719.

Tamarov K., Nakki S., Xu W., Lehto V.P. (2018). Approaches ti Improve The Biocompatibility and Systemic Circulation of Inorganic Porous Nanoparticles. *Journal of Materials Chemistry B*. 6, 22, 3632–3649.

UllahvF., Shah K.U., Nawaz A., Nawaz T., Khan K.A., Alserihi R.F., Tayeb H.H., Tabrez S., Alfatama M. (2022). Synthesis, Characterization and In Vitro Evaluation of Chitosan Nanoparticles Physically Admixed With Lactose Microspheres for Pulmonary Delivery of Montelukast. *Polymers*. 14, 17, 14173564.

Veiga E., Ferreira L., Correia M., Pires P., Hameed H., Araujo A., Cefali L., Mazzola P., Hamishehkar A., Veiga F., Paiva-Santos A. (2023). Anti-aging peptides for advanced skincare: Focus on nanodelivery systems. *Journal of Drug Delivery Science and Technology*. 89, 105087.

Vithoba S.R., Velraj M. (2023). Optimization, Formulation and Characterization of Nano Based TDDS of Eplerenone. International Journal of Applied Pharmaceutics. 15, Issue 1, 227 – 233.

Wani S., Ali. M., Mehdi S., Masoodi M., Zargar M., Shakeel F. (2023). A review on chitosan and alginate-based microcapsules: Mechanism and applications in drug delivery systems. International Journal of Biological Macromolecules. 2481, 125875.

Wang Y., Qiu F., Zheng Q., Hong A., Wang T., Zhang J., Lin L., Ren Z., Qin T. (2024). Preparation, characterization and immune response of chitosan-gold loaded Myricaria germanica polysaccharide. International Journal of Biological Macromolecules. 257, 128670.

Waqas M.K., Safdar S., Buabeid M., Ashames A., Akhtar M., Murtaza G. (2022). Alginate-Coated Chitosan Nanoparticle for pH-dependent Release of Tamoxifen Citrate. Journal of Experimental Nanosciences. 17, 1, 522-534.

Wang J., Liu D., Guan S., Zhu W., Fan L., Zhang Q., Cai D. (2020). Hyaluronic Acid Modified Liposomal Honokial Nanocarrier : Enhacer Anti-Metastasis and Antitumor Efficacy Against Breast Cancer. Carbohydrate Polymers. 235, 115981.

Weng J., Tong H.H.Y., Chow S.F. (2022). Invitro Release Study of The Polymeric Drug Nanoparticles : Development and Validation of a Novel Method. Pharmaceutics. 12, 8, 732.

Wathoni N., Rusdin A., Febriani E., Purnama D., Daulay W., Azhary S.Y., Panatarani C., Joni I.M., Lesmana R., Keiichi M., Muchtaridi M. (2019). Formulation and Characterization of Alfa Mangostin in Chitosan Nanoparticles Coated by Sodium Alginate, Sodium Silicate and Polyethylene Glycol. Journal of Pharmacy and Bioallied Scinces. 20, 20, 1-9.

Yubia A.D.F., Elizabeth C.M., Alma C.M., Jaime L.M., Agustin R.C., Judith T.C., Anna Luisa L.M. (2021). Polysaccharide-Based Nanoparticles for Colon-Targeted Drug Delivery Systems. Polysaccharides. 2, 3, 626-647.

Yu Y., Wang C., Fu, Q., Wan Y., Yu A. (2024). Multi-crosslinked hydrogel built with hyaluronic acid-tyramine, thiolated glycol chitosan and copper-doped bioglass nanoparticles for expediting wound healing. Carbohydrate Polymers. 3271, 21635.

Zhu D., Ma W., Yang M., Cheng S., Zhang L., Du M. (2024). Protection of osteogenic peptides in nanoliposomes: Stability, sustained release, bioaccessibility and influence on bioactive properties. Food Chemistry. 43615, 37683.